Biochar from Orange (*citrus sinensis*) Peels by Acid Activation for Methylene Blue Adsorption

Jawad, Ali H.*[+]

School of Chemistry and Environment, Faculty of Applied Sciences, Universiti Teknologi MARA, 40450 Shah Alam, Selangor, MALAYSIA

Al-Heetimi, Dhafir T.A.

Department of Chemistry, College of Education for Pure Science Ibn-Al Haitham, Baghdad University, IRAQ

Mastuli, Mohd Sufri[•]

School of Chemistry and Environment, Faculty of Applied Sciences, Universiti Teknologi MARA, 40450 Shah Alam, Selangor, MALAYSIA

ABSTRACT: *In this work, orange (Citrus sinensis) peels biochar (OPBC) were prepared by one-step H_2SO_4 activation for Methylene Blue (MB) adsorption from aqueous solution. The physicochemical properties of OPBC were characterized using instrumental analyses such as CHNS-O analyzer, Fourier Transform InfraRed (FT-IR) spectroscopy, Scanning Electron Microscopy (SEM), X-Ray Diffraction (XRD), and point-of-zero charge (pH_{pzc}) analysis. Batch mode adsorption study was conducted by varying operational parameters such as adsorbent dosage (0.02 – 0.20 g), solution pH (3 – 11), initial MB concentrations (50 – 300 mg/L), and contact time (0 – 1440 min). The equilibrium data was found to better fit with the Langmuir isotherm model compare to Freundlich and Temkin models. The maximum adsorption capacity, q_{max} of OPBC for MB adsorption was 208.3 mg/g at 303 K. The kinetic study revealed that the present system obeyed Pseudo-Second-Order (PSO), model. The thermodynamic adsorption parameters such as standard enthalpy (ΔH°), standard entropy (ΔS°), and standard free energy (ΔG°) showed that the adsorption of MB onto OPBC surface endothermic in nature and spontaneous under the experimental conditions. All above-mentioned results indicate that the OPBC can feasibly employ for the elimination of MB from aqueous solution.*

KEYWORDS: *Biochar; Orange peel; Chemical activation; Adsorption; Methylene blue*.

INTRODUCTION

Wastewater pollution by dyeing industries, such as textile and printing has been identified to cause environmental problems in aquatic environments. Uncontrolled release of dyes into effluents is a major concern since most of these dyes are highly visible, stable and resistant to chemical, photochemical as well as biological degradation [1]. Basic dyes are cationic species charged sites that reside on heteroatoms such as nitrogen or sulfur atoms. Such basic dye species present an obvious coloration even at low concentration (< 1 mg/L)

** To whom correspondence should be addressed.*

+ E-mail: ahjm72@gmail.com ; ali288@salam.uitm.edu.my

• Other Address: Centre for Nanomaterials Research, Institute of Science, Uviversiti Teknologi MARA, 40450 Shah Alam, Selangor, MALAYSIA

1021-9986/2019/2/91-105 15/$/6.05

and are classified as toxic colorants [2]. Methylene Blue (MB) is a basic dye with favourable water solubility that is used in industrial activities such as dyeing of textiles and leather, printing calico, printing cotton, and biological staining methods [3]. The acute exposure to MB dye may cause eye irritation, gastrointestinal irritation, and nausea upon ingestion, including vomiting and diarrhea [4].

Several methods have been reported for the removal of dyes from industrial effluents and wastewaters, including bioremediation [5], electrochemical degradation [6], cation exchange membranes [7], Fenton chemical oxidation [8], and photocatalysis [9, 10]. Comparatively, the adsorption process is recognized as a promising and the most widely used technique in the wastewater treatment processes. Adsorption-based treatment with appropriate adsorbent materials displays high performance and selectivity, flexibility and simplicity of design, convenience of operation without producing harmful by-products as well as economically cost effective [11].

Activated Carbon (AC) is known to be a very effective adsorbent material due to its high surface area, variable pore structure, micro-porous structure, high adsorption capacity and occurrence of various surface functional groups [12]. These unique characteristics make AC very versatile material to remove a wide variety of pollutants such as dyes, heavy metals, pesticides, and gases. However, its use is limited because of its high cost. This has led to research and develop of carbonaceous adsorbents from agricultural waste peels due to the precursors are eco-friendly, cheap, renewable, safe, and abundant. In recent years, researchers had studied the production of ACs from fruit and vegetable peels as cheap and renewable precursors, such as jackfruit peel [13], mangosteen peel [14], pineapple peel [15], citrus fruit peel [16], potato peel [17], rambutan peel [18], pomegranate peel [19], grapefruit peel [20], cassava peel [21], Cucumis sativus peel [22], pomelo peel [23], banana peel [24], guava peel [25], mandarin peel [26], and mango peel [27].

Orange, specifically known as *Citrus sinensis*, is one of the most famous subtropical fruits in the world. The outer pericarp is orange when ripe, while the inner mesocarp is white, spongy, and non-aromatic [28]. Orange fruit is primarily eaten fresh and available as food complements in desserts, salads, gelatins, fruit cocktail, jam, or juice combinations in the citrus processing industries [29]. In 2010, the annual production of orange fruit is projected at 64 million MT, translating to approximately 32 million MT of peels as the byproducts [30]. In fact, Orange Peels (OP) are natural, eco-friendly and low-cost precursors of Activated Carbon (AC), which can be utilized in the removal of diverse types of aquatic pollutants and also reduce pollution. Being a renewable resource, OP can be considered as a promising precursor for producing high quality activated carbon suitable for environmental technology if applied in the treatment of water and wastewater.

The adsorption properties of carboneous materials strongly depend on the nature and preparation of the source materials including the activation steps, such as physical or chemical activation. Physical activation is a two-step process where conversion of the precursor into carbonized material (char) is followed by activation with an oxidizing gas such as carbon dioxide, water vapor or their mixtures [31]. In chemical activation, the precursor is impregnated with dehydrating chemical agents and carbonization at variable temperatures [32]. Chemical activation has some advantages since it employs lower temperatures and has a higher carbonization yield than physical activation [33]. Sulphuric acid (H_2SO_4) is frequently used as a low cost activator for the preparation of carbon adsorbents from ligno-cellulosic products. H_2SO_4 gives the possibility to develop porous structure by degrading cellulosic material in plant materials and the aromatization of the carbon skeleton [34]. H_2SO_4 has been frequently used as an activation agent to produce AC from different biomass sources such as euphorbia rigida [34], bagasse [35], almond husk [36], agricultural waste (Parthenium hysterophorus) [37], sunflower and oil cake [38], pine-fruit shell [39], delonix regia pods [40], wild carrot [41], coconut leaves [42], potato peel and neem bark [43].

To the best of our knowledge, the development of biochar from OP by chemical activation with H_2SO_4 has not yet been addressed by researchers. Thus, in this work, OP was used as a renewable, naturally abundant, inexpensive, and eco-friendly precursor preparing orange peel biochar (OPBC) by a single by a single step treatment with H_2SO_4 activation, which has the advantages of shorter time and low energy consumption. The adsorptive properties of the obtained OPBC have been tested

for attraction of a hazardous cationic dye such as MB. The adsorption performance of OPBC towards MB has been extensively tested at different experimental conditions. The equilibrium isotherms and kinetics of OPBC adsorption system have been determined and analyzed using several adsorption models. Furthermore, the surface characteristics and morphology of OPBC have been identified.

EXPERIMENTAL SECTION

Adsorbate (MB)

Methylene Blue (MB) was purchased from R&M Chemicals, Malaysia with the chemical formula ($C_{16}H_{18}ClN_3S.xH_2O$) and molecular weight (319.86 g/mol). The chemicals such as sulphuric Acids (95-98%), hydrochloric acids, sodium hydroxide were analytical grade and purchased from HmbG Company. Ultra-pure water was used to prepare all solutions.

Preparation and characterization of OPAC

Orange Peels (OP) used for preparation biochar was collected from the local fresh juice shop in Penang, Malaysia. OP was firstly washed with water and subsequently dried at 105°C for 24 h to remove the moisture contents. The dried OP was ground and sieved to the size of 1–2 mm before mixing with concentrated H_2SO_4 (95–98%)(). The mixing ration was fixed at 1 g of dried OP powder with 1 mL of concentrated H_2SO_4 according to the method reported by *Garg et al.* [44]. The OPBC product was ground and sieved to obtain a powder with a particle size range of 250–500 μm. The yield of OPBC was calculated according to a published method [45], and the bulk density was determined by following the method reported by *Ahmedna et al.* [46]. The moisture content was determined by an oven drying method [47], where the ash content determination used standard methods [48]. The iodine number is a measure of micropore content (0–20Å) and was obtained by a standard method [49]. The proximate analysis of the OPBC was performed using a muffle furnace and the elemental analysis was carried out using a CHNS-O analyzer (Perkin-Elmer, Series II, 2400). The functional groups of OPBC before and after MB adsorption were measured by Fourier Transform InfraRed (FT-IR) Spectroscopy (Perkin-Elmer, Spectrum RX I), with a spectral range from 4,000 cm^{-1} to 400 cm^{-1}. The surface morphology of OPBC before and after adsorption of MB was measured by using a Scanning Electron Microscope (HITACHI, TM3O3OPlus, Tabletop Microscope). X-Ray Diffraction (XRD) analysis was performed on coal in order to determine the crystallinity or amorphous nature before and after the activating process by X-Ray Diffraction (XRD) in reflection mode (Cu Kα radiation) on a PANalytical, X'Pert Pro X-ray diffractometer. Scans were recorded with a scanning rate of 0.59°/s. The diffraction angle (2θ) was varied from 10º to 90º. The pH at the *point-of-zero* charge (pH_{pzc}) was estimated by using a pH meter (Metrohm, Model 827 pH Lab, Switzerland), as described elsewhere [50].

Batch adsorption experiments

The batch adsorption experiments of MB onto OPBC were carried out in a series of 250 mL Erlenmeyer flasks containing 100 mL of MB solution. The flasks were capped and agitated in an isothermal water bath shaker (Memmert, waterbath, model WNB7-45, Germany) at the fixed shaking speed of 110 strokes/min and 303 K until equilibrium was attained. Batch adsorption experiments were carried out by varying several experimental variables such as adsorbent dosage (0.02 to 0.2 g), pH (3 to 11), initial dye concentration (50 to 300 mg/L) and contact time (0 to 1440 min) to determine the optimum adsorption conditions for MB. The pH of MB solution was adjusted by adding either 0.10 mol/L HCl or NaOH. After mixing the OPBC-MB system, the supernatant was collected with a 0.20 μm Nylon syringe filter and the concentrations of MB were monitored at a different time interval using a HACH DR 2800 Direct Reading Spectrophotometer at the maximum wavelength (λ_{max}) of absorption at 661 nm. For the thermodynamic studies, similar procedures were applied at 313, 323, and 333 K, with the other variables, held constant. The blank test was carried out in order to account for colour leached by the adsorbent and adsorbed by the glass containers, blank runs with only the adsorbents in 100 mL of doubly distilled water and 100 mL of dye solution without any adsorbent were conducted simultaneously at similar conditions. The adsorption capacity at equilibrium, q_e (mg/g) and the percent of colour removal, CR (%) of MB were calculated using Eqs. (1) and (2).

$$q_e = \frac{(C_o - C_e)V}{W} \quad (1)$$

Table 1: Physicochemical characteristics of the OPBC.

Typical properties	Values
Bulk density (g/mL)	0.6
Iodine number (mg/g)	521
Proximate analysis (wt. %)	
Ash content	4.0
Moisture content	1.6
Fixed carbon (yield)	53.8
Ultimate analysis (wt. %)	
C	48.80
H	3.09
N	1.42
S	0.13
O (by difference)	46.56

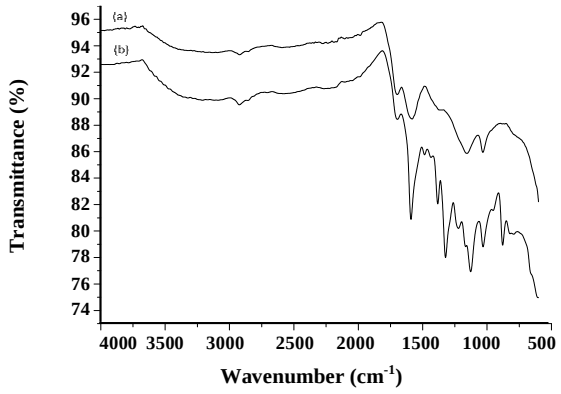

Fig. 1: FTIR spectra of OPAC: (a) before MB adsorption, and (b) after MB adsorption.

$$CR\% = \frac{(C_o - C_e)}{C_o} \times 100 \quad (2)$$

Where C_o is the initial dye concentration (mg/L); *Ce* is the dye concentration at equilibrium (mg/L); *V* is the volume of dye solution (mL), and W is the dry mass of the adsorbent (g).

RESULTS AND DISCUSSION

Characterization of OPBC

Physical properties

The results of the physical characterization of OPBC are recorded in Table 1. The ultimate results indicate that OPBC has a relatively high carbon and oxygen content. It was reported by values of bulk density, ash content, and moisture content, along with a relatively high yield of carbon.

FT-IR spectral analysis

The pattern of adsorption onto biomass materials is related to the availability of active functional groups and bonds of the AC surface. For the elucidation of these active sites, FT-IR spectral analysis was performed. Several IR bands appeared in the FT-IR spectrum of OPBC before adsorption (Fig. 1a) that were assigned to various functional groups, in accordance with their respective wavenumber (cm^{-1}) position as reported in the literature. The weak band observed around 2900 cm^{-1} is assigned to the aliphatic C–H stretching (methine, methyl and methylene groups of side chains) [51]. The band at about 1700 cm^{-1} relates to C=O stretching of ketones, aldehydes, lactones or carboxyl groups, and the band at 1600–1580 cm^{-1} is assigned to C=C vibrations in aromatic rings [52]. The IR bands between 1300 and 1000 cm^{-1} are observed for oxidized carbon materials and are assigned to C–O and/or C–O–C stretching in acids, alcohols, phenols, ethers and/or esters groups and sulphonic acid groups ($-SO_3$) [53, 54]. Thus, the FT-IR spectrum of OPBC before adsorption indicates that the external surface of OPBC is rich in various functional groups, containing oxygen of carboxylic and carbonyl species. After adsorption of MB, the spectrum of OPBC (Fig. 1b) shows attenuated band intensity where the functional groups either shifted in frequency or disappear in some cases when MB molecules are bound onto the OPBC surface. These spectral changes indicate the possible involvement of those functional groups on the surface of OPBC in the adsorption process.

Surface morphology of OPBC

The changes in the surface morphology of OPBC before and after MB adsorption were observed by comparing their SEM images. Fig. 2a shows the surface property of OPBC, which is seen as a rough and irregular surface along with heterogeneous cavities that well distributed across the OPBC surface. The surface morphology of OPBC after MB adsorption (Fig. 2b) reveals a change in the topography of the adsorbent, as evidenced by the appearance of reduced pore structure

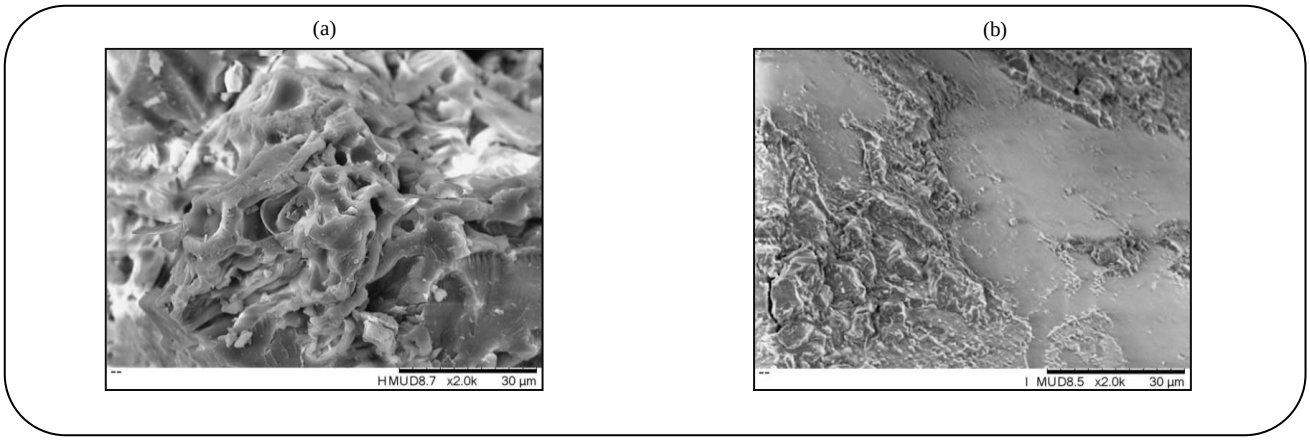

Fig. 2: SEM micrograph of OPBC particle (at 2.0K magnifications): (a) before MB adsorption, and (b) after MB adsorption.

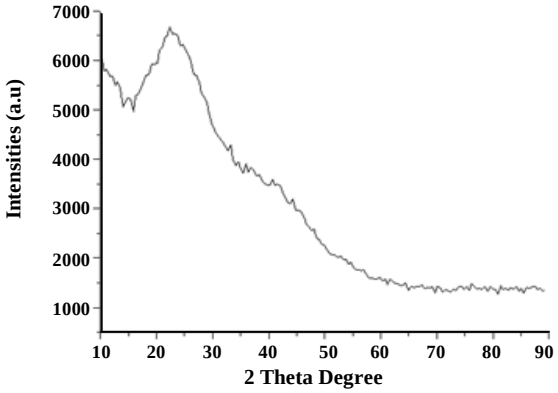

Fig. 3: XRD pattern of OPBC.

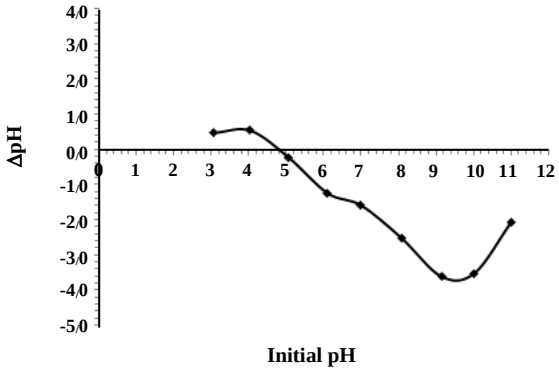

Fig. 4: pHpzc of OPBC suspensions.

and smoother surface features due to the adsorption of MB onto OPBC surface [55, 56].

XRD analysis of OPBC

XRD patterns of the sample are shown in Fig. 3. XRD pattern shows a broad hump indicating that the carbon sample is amorphous in nature. However, a second hump around 40º indicates that there exists a short-range crystallographic ordering in the sample. No sharp peaks indicate an amorphous nature of OPBC as observed from the XRD pattern.

Point-of-Zero Charge (pH_{pzc})

Fig. 4 shows the pH_{pzc} results of the experiments performed with the OPBC, where the pH ranged from 2 to 11. The pH_{pzc} of the OPBC was 4.80, which indicates the acid character of the OPAC surface, in agreement with the presence of acid groups from the FT-IR results (Fig. 1a). Generally, adsorption of anions is favored at solution pH below the pH_{pzc} value as the surface of OPBC is positively charged due to protonation whereas at solution pH above the pH_{pzc} value, the surface of OPBC becomes negatively charged and thus, adsorption of cations is preferred. In this respect, *Karagöz et al.* [38] reported that the pH_{pzc} value lies between pH 2.5 and 5.5 which was attributed to the acid form of AC derived from sunflower oil cake treated with H_2SO_4.

Adsorption of MB

Effect of the adsorbent dosage

The effect of adsorbent dosage on the removal of the MB from aqueous solution was determined by using variable quantities of OPBC adsorbent ranging from 0.02 to 0.20 g at fixed volumes (100 mL) and initial dye solution where C_o was 100 mg/L. For these experiments, other operation parameters were held constant at 303 K, shaking speed of 110 stroke/min, the contact time of 60 min, and an unadjusted pH at 5.60 for the initial MB solution. The results are shown in Fig. 5. The highest level of

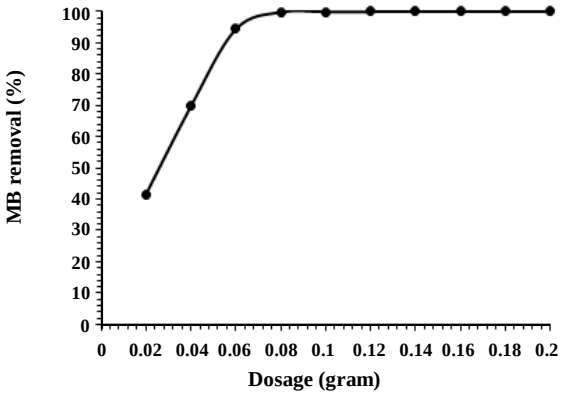

Fig. 5: Effect of OPAC dosage on MB removal (%) at [MB]$_o$ = 100 mg/L, V = 100 mL, pH= 5.6, T = 303 K, shaking speed = 110 stroke/min, and contact time =1440 min.

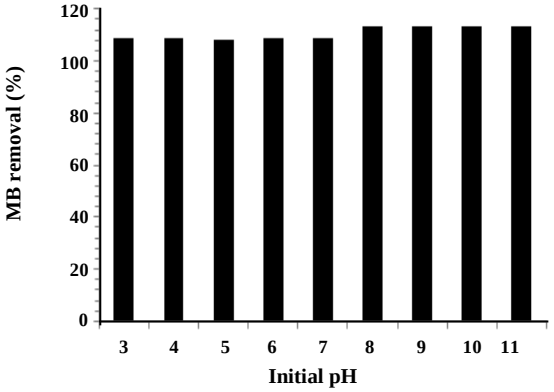

Fig. 6: Effect of pH on the adsorption capacity of MB by OPAC at [MB]$_o$ = 100 mg/L, V = 100 mL, T = 303 K, shaking speed = 110 stroke/min, contact time = 1440 min and OPBC dosage = 0.08 g.

MB removal was achieved using 0.08 g OPBC and further addition has not significantly affected the MB removal. The observed increase in the dye removal (%) with adsorbent dosage was attributed to an increase in the available adsorbent surface area, as the number of adsorption sites increases correspondingly. However, no significant changes in MB removal were observed beyond 0.08 g/ 100 mL OPBC dose. Due to conglomeration of adsorbent particles, there is no increase in effective surface area of OPBC. Therefore, 0.08 g of OPBC was selected for subsequent work.

Effect of pH

The pH of the solution influences the speciation of the dyes, along with the surface charge of the adsorbent. Fig. 6 shows the effect of variable pH from 3 to 11 on the adsorption capacity with MB. from 3 up to 5, where no remarkable change was observed by increasing the pH to an alkaline environment. MB uptake (q_e) onto OPBC was not affected by pH within the range from 3 to 11 due to the buffering effect of the adsorbent [57]. Similar observations have been reported for the adsorption of MB by activated carbon developed from coconut leaves by H_3PO_4 activation [52], and KOH activation [53]. Therefore, the pH value of unadjusted MB solution (pH 5.6) was used throughout this study.

Effect of initial dye concentration and contact time

The experimental results for the adsorption properties of MB onto OPBC at various initial concentrations are shown in Fig. 7. The amount of MB adsorbed by the OPBC adsorbent at equilibrium increased rapidly from 62.6 to 196.9 mg/g as the initial dye concentration increased from 50 to 300 mg/L. Indeed, the resistance to mass transfer between the solid and aqueous phase is more easily overcome due to the driving forces. The effect can be attributed to the greater rate of collision rate between MB and OPBC surface at higher initial dye concentration. Hence, additional amounts of MB were transferred to the OPBC surface. Additional time was needed to reach equilibrium for higher dye concentration because there was a tendency for MB to penetrate deeper within the interior surface of the OPBC and be adsorbed at active pore sites. This indicates that the initial dye concentration plays a significant role in the adsorption capacity of MB onto OPBC sorbent.

Effect of temperature on dye adsorption

Temperature is anticipated to have an influence on the dye adsorption properties of OPBC adsorbent with MB. The effect of temperature on the dye adsorption properties at 313, 323, and 333 K with fixed initial MB concentration of 50 mg/L was investigated, as shown in Fig. 8. The adsorption capacity of the OPBC increased when the temperature increased from 313 to 333 K. The uptake of MB onto AC was rapid initially and then slows down gradually until equilibrium was attained, after that there was not significantly increased in the MB uptake. The observed result indicates that the adsorption process

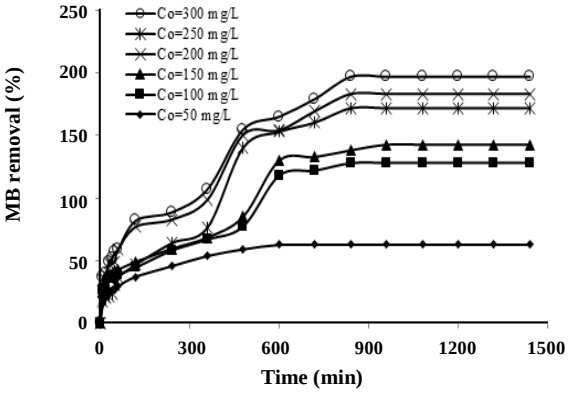

Fig. 7: Effects of initial concentration and contact time on the adsorption of MB by OPBC (V = 200 mL, T = 303 K, pH = 5.6, shaking speed = 110 stroke/min, and OPAC dosage = 0.16 g).

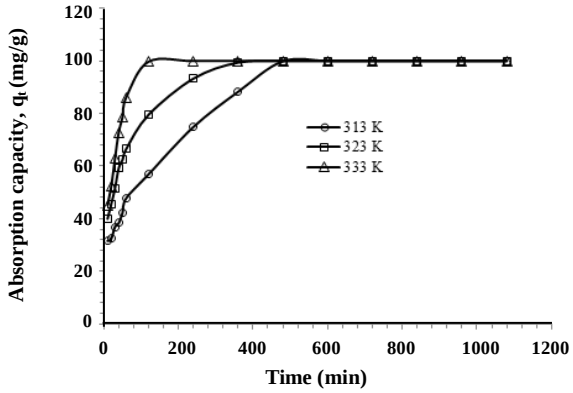

Fig. 8: Effects of temperature on the adsorption of MB by OPBC (V = 200 mL, pH = 5.6, shaking speed = 110 stroke/min, and OPAC dosage = 0.16 g).

of MB onto OPBC was favoured at a higher temperature, in agreement with an endothermic adsorption process. This can be partly attributed to strong attractive forces between MB and AC at higher temperatures [58], along with the contributions due to desolvation of the OPBC surface. It can also be said that reaction of dye molecules and surface functional groups is enhanced by increased temperature of reaction [59].

Adsorption isotherm

The adsorption isotherm results for OPBC were fitted using three types of isotherm models, which are Langmuir, Freundlich, and Temkin to evaluate the suitable model for describing the adsorption process. Adsorption isotherm reveals the relationship between the mass of adsorbate adsorbed per unit weight of adsorbent at equilibrium and liquid-phase equilibrium concentration of the adsorbate [60]. The Langmuir model assumes that the adsorptions occur at specific homogeneous sites on the adsorbent. As well, monolayer adsorption occurs onto a surface containing a finite number of adsorption sites with uniform adsorption and no transmigration of adsorbate on an idealized planar surface. The data of the equilibrium studies for the adsorption of MB dye onto OPBC may follow the Langmuir model [61] as in Eq. (3):

$$\frac{C_e}{q_e} = \frac{1}{q_{max} k_L} + \frac{1}{q_{max}} C_e \qquad (3)$$

where C_e is the equilibrium concentration (mg/L) and q_e is the amount of adsorbed species per specified amount of adsorbent (mg/g), k_L is the Langmuir equilibrium constant and q_{max} is the amount of adsorbate required to form an adsorbed monolayer. Hence, a plot of C_e/q_e vs. C_e should be a straight line with a slope ($1/q_{max}$) and an intercept ($1/q_{max}.k_L$) as shown in Fig. 9a. The essential characteristics of Langmuir isotherm can be expressed by a dimensionless separation factor (R_L) [62], defined by Eq. (4):

$$R_L = \frac{1}{1 + k_L C_0} \qquad (4)$$

An adsorption system is considered favourable when $0 < R_L < 1$, unfavourable when $R_L > 1$, linear when $R_L = 1$ or irreversible when $R_L = 0$. By contrast, the Freundlich model [63] assumes heterogeneous surface energies, as described by a form of the Langmuir equation that varies as a function of the surface coverage. This model is presented as Eq. (5):

$$\ln q_e = \ln k_F \frac{1}{n} \ln C_e \qquad (5)$$

Where C_e is the equilibrium concentration of the adsorbate (mg/L), q_e is the amount of adsorbate adsorbed per unit mass of adsorbent (mg/g). The affinity constant k_F (mg/g (l/mg)$^{1/n}$, relates to the adsorption capacity of the adsorbent and n is the constant where indicates the relative favourability of the adsorption process. Thus, a plot of $ln\ q_e$ vs. $ln\ C_e$ should be a straight line with a slope $1/n$ and an intercept of $ln\ k_F$ (Fig. 9b). Temkin model [64] considered the effects of indirect adsorbate/adsorbate interactions on adsorption isotherms. The Temkin isotherm can be expressed in its linear form as in Eq. (6):

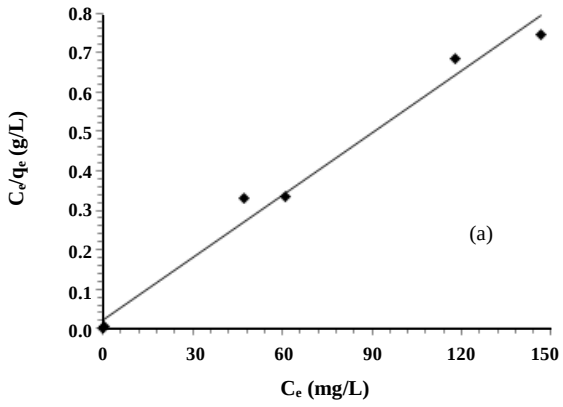

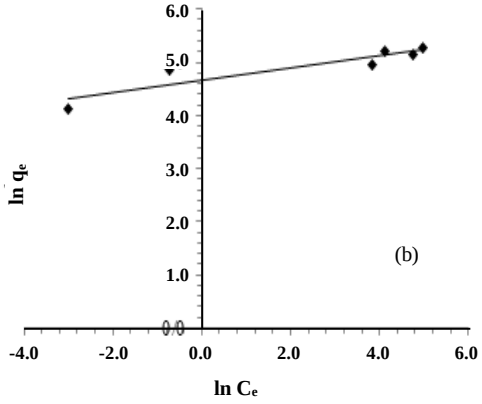

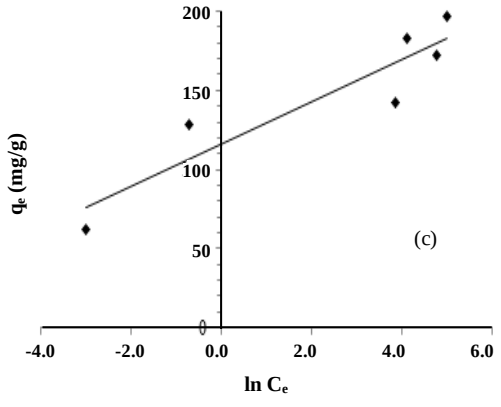

Fig. 9: Isotherm profiles for the adsorption of MB onto OPBC: (a) Langmuir isotherm, (b) Freundlich isotherm, and (c) Temkin isotherm at 303 K.

$$q_e = B\ln k_T + B\ln C_e \quad (6)$$

Where B = (RT/b), a plot of q_e versus $ln\ C_e$ yielded a linear line enables to determine the isotherm constants k_T and B (Fig. 9c). k_T is the Temkin equilibrium binding constant (L/mg) that corresponds to the maximum binding energy, and constant B is related to adsorption heat. The adsorption heat of all the molecules in the layer is expected to decrease linearly with coverage because of adsorbate/adsorbate interactions. The related parameters were calculated, and the results are shown in Table 2. Basd on calculated data, Langmuir model fits the data better than the Freundlich, and Temkin models. This result is confirmed by the high R^2 value for the Langmuir model (0.983) compared with the Freundlich (0.841), and Temkin (0.859) models. Langmuir isotherm indicates the surface homogeneity of the adsorbent. The adsorbent surface is made up of small adsorption patches, which are energetically equivalent to each other in terms of adsorption phenomenon.

The monolayer adsorption capacity (q_{max}) for OPBC with MB was compared with other types of H_2SO_4–treated biomass in Table 3. In this work, the values of RL obtained were between 0 and 1 and indicate that the adsorption process is favourable for the OPBC–MB system. The calculated RL values at different initial MB concentrations are shown in Table 4.

Kinetic studies

The Pseudo-First-Order (PFO) model and Pseudo-Second-Order (PSO) model were used to investigate the adsorption kinetics of MB dye on OPAC. The PFO was originally proposed by Lagergren [66] and its linearized form is given by Eq. (7):

$$\ln(q_e - q_t) = \ln q_e - k_1 t \quad (7)$$

Where q_e is the amount of solute adsorbed at equilibrium per unit weight of adsorbent (mg/g), q_t is the amount of solute adsorbed at any time (mg/g), and k_1 is the adsorption constant. This expression is the most popular form of PFO model. k_1 values at different initial MB concentrations were calculated from the plots of $ln\ (q_e-q_t)$ vs. t (Fig. 10a) and the values are given in Table 6. The linear form of the PSO model is given by Eq. (8) [67]:

$$\frac{t}{q_t} = \frac{1}{k_2 q_e^2} + \frac{t}{q_e} \quad (8)$$

Table 2: Isotherm parameters for adsorption of MB by OPBC at 303 K.

Isotherm	Parameter	Value
Langmuir	q_m (mg/g)	208.3
	k_L (L/mg)	1.04
	R^2	0.9975
Freundlich	K_F [(mg/g) (L/mg)$^{1/n}$]	160.9
	n	0.11
	R^2	0.7009
Temkin	B	16.5
	k_T (L/mg)	2.09
	R^2	0.9282

Table 3: Comparative of adsorption capacities for MB onto different treated biomass wit H_2SO_4

H_2SO_4-treated biomass	Adsorbent dosage, g	pH	Temp. (K)	q_{max} (mg/g)	References
Oragne Peel Biochar (OPBC)	0.08 g / 100 mL	8	303	208.3	This study
Pine-fruit shell	0.3 g/ 100 mL	8.5	298	529	[39]
Mango peels	0.14 g / 100 mL	5~6	303	277.8	[27]
Coconut leaves	0.15 g / 100 mL	6	303-323	126.9 – 149.3	[42]
Euphorbia rigida	0.2 g/ 100 mL	6	293–313	114	[34]
Bagasse	0.4 g/ 100 mL	9	300–333	49.8–56.5	[35]
Ficus carica	0.5 g/ 100 mL	8	298–323	47.6	[65]
Parthenium hysterophorus	0.4 g/ 100 mL	7	298	39.7	[37]
Delonix regia pods	0.2 g/ 100 mL	7	298	23.3	[40]
Wild carrot	0.05 g / 100 mL	6	298	21	[41]
Sunflower oil cake	0.2 g/ 100 mL	6	288–318	16.4	[38]

Table 4: Dimensionless constant separation factor, R_L for adsorption of MB onto OPAC at various initial concentrations.

Parameter	Concentrations, C_o (mg/L)					
R_L	50	100	150	200	250	300
	0.078	0.041	0.027	0.021	0.017	0.014

Where, the PSO rate constant (k_2; g/mg min) and $q_{e,cal}$ were calculated from the intercept and slope of t/q_t vs. t, shown in Fig. 10b. In Table 6, the observed R^2 values are nearly unity ($R^2 \geq 0.99$) for the PSO kinetic model, where the values of $q_{e,cal}$ are in good agreement with $q_{e,exp}$.

Adsorption thermodynamics

The thermodynamic adsorption parameters of MB onto OPBC were computed from the experimental data obtained at 313, 323, and 333 K. Gibb's free energy (ΔG°), enthalpy (ΔH°) and entropy (ΔS°) were calculated using the following equations (9 to 11) [68]:

$$k_d = \frac{q_e}{C_e} \quad (9)$$

$$\Delta G^\circ = \Delta H^\circ - T\Delta S^\circ \quad (10)$$

$$\ln k_d = \frac{\Delta S^\circ}{R} - \frac{\Delta H^\circ}{RT} \quad (11)$$

Table 6: PFO and PSO kinetic parameters and their corresponding values at different initial dye concentrations by OPBC.

Parameters	Concentration, C_o (mg/L)					
	50	100	150	200	250	300
$q_{e,exp}$ (mg/g)	61.5	122.5	170.9	191.5	206.1	236.9
	PFO					
$q_{e,cal}$ (mg/g)	32.4	146.5	158.7	233.4	204.3	216.9
$k_{1\times10^{-3}}$(1/min)	9.0	7.5	5.5	3.9	2.8	1.6
R^2	0.967	0.791	0.9770	0.660	0.981	0.938
	PSO					
$q_{e,cal}$ (mg/g)	58.5	119.1	169.5	188.5	208.1	238.1
k_2 x 10^{-3}(g/mg min)	1.5	0.145	0.0576	0.0588	0.024	0.017
R^2	0.989	0.966	0.970	0.908	0.939	0.914

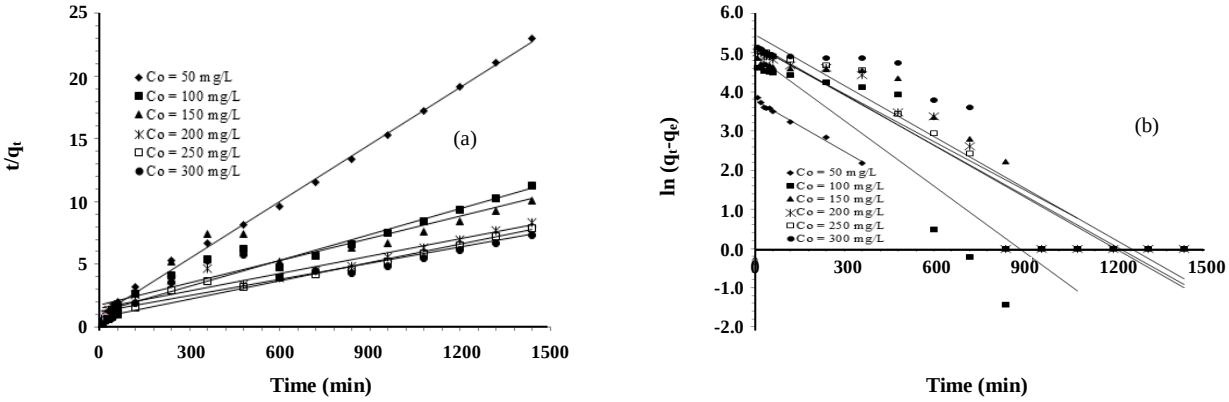

Fig. 10: Kinetic profiles for the adsorption of MB onto OPBC at variable temperatures: (a) PFO and (b) PSO.

Where k_d is the distribution coefficient, q_e is the concentration of MB adsorbed on OPBC at equilibrium (mg/L), C_e is the equilibrium concentration of MB in the liquid phase (mg/L), R is the universal gas constant (8.314J/mol.K) and T is the absolute temperature (K). The values of ΔH° and ΔS° were calculated from the slope and intercept of van't Hoff plots of *ln* k_d versus *1/T* respectively (Fig. 11). The thermodynamic parameters are listed in Table 7. In general, the value for ΔG°, energy for physisorption ranges from -20 to 0 kJ/mol, the physisorption together with chemisorption fall at the range of -20 to -80 kJ/mol and chemisorption is more negative in magnitude with a range of -80 to -400 kJ/mol [69]. The negative values of ΔG° indicate spontaneous and favorable MB adsorption onto the surface of OPBC [70]. The enthalpy for physisorption is generally below 0 kJ/mol, while for the chemisorption is a more negative range (80-420 kJ/mol) of values [67]. The positive value of the enthalpy change (ΔH° = 67.646 kJ/mol) indicates that the adsorption process is an endothermic and this value also shows that the adsorption follows a chemisorption mechanism in nature involving strong forces of attractions [71]. The positive entropy change (ΔS°) value of 281.761 J/mol.K confirms a high preference of MB molecules for the carbon surface of OPAC and also suggests the possibility of some structural changes or readjustments in the dye-carbon adsorption complex [72]. It also corresponds to an increase in the degree of freedom of the adsorbed species due to adsorbate disorder and/or loss of water upon binding of MB to the OPAC surface [73].

CONCLUSIONS

From the results of the current work, it can be concluded that liquid phase H_2SO_4 treatment of orange peel biomass waste promotes the formation of biochar

Table 7: Thermodynamic parameters values for the adsorption of MB onto OPBC.

Temperature (K)	Thermodynamics			
	k_d	ΔG° (kJ/mol)	ΔH° (kJ/mol)	ΔS° (J/mol K)
313	2961.2	-20.5	67.6	281.7
323	4898.7	-12.9		
333	14198.7	-15.4		

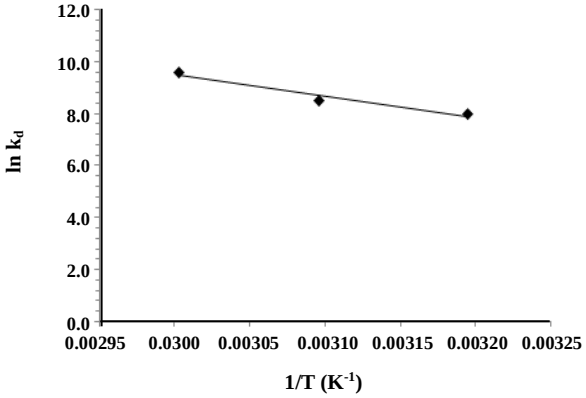

Fig. 11: Plot of ln k_d vs. 1/T for calculation of thermodynamic parameters for the adsorption of MB onto OPBC.

to act as a low-cost and renewable adsorbent for the removal of MB dye from aqueous solutions. The adsorption experiments indicated that the pseudo-second-order model provided the best description of the kinetic uptake properties, while adsorption results at equilibrium are described by the Langmuir model where the maximum adsorption capacity (q_{max}) is 208.3 mg/g. The thermodynamic parameters indicate that the adsorption process is endothermic in nature and driven by entropy to yield a spontaneous adsorption process. The results indicated that OPAC is an efficient adsorbent for MB adsorption.

Acknowledgements

The authors would like to thank the Institute of Research Management and Innovation (IRMI) for funding this research work under the Geran Insentif Penyeliaan (GIP) (600-IRMI/My/RA 5/3/GIP (055/2017)).

Received : Oct. 5, 2017 ; Accepted : Apr. 9, 2018

REFERENCES

[1] Mubarak N.S.A., Jawad A.H., Nawawi W.I., Equilibrium, Kinetic and Thermodynamic Studies of Reactive Red 120 Dye Adsorption by Chitosan Beads From Aqueous Solution, *Energ. Ecol. Environ.*, **2**: 85–93 (2017).

[2] Jawad A.H., Alkarkhi A.F.M., Mubarak N.S.A., Photocatalytic Decolorization of Methylene Blue by an Immobilized TiO_2 Film Under Visible Light Irradiation: Optimization Using Response Surface Methodology (RSM), *Desalin. Water Treat.*, **56**: 161–172 (2015).

[3] Jawad A.H., Mubarak N.S.A., Ishak M.A.M., Ismail K., Nawawi W.I., Kinetics of Photocatalytic Decolourization of Cationic Dye Using Porous TiO_2 Film, *J. Taibah Univ. Sci.*, **10**: 352–362 (2016).

[4] Jawad A.H., Rashid R.A., Mahmuod R.M.A., Ishak M.A.M., Kasim N.N., Ismail K., Adsorption of Methylene Blue onto Coconut (*Cocos Nucifera*) Leaf: Optimization, Isotherm and Kinetic Studies, *Desalin. Water Treat.*, **57**: 8839–8853 (2016).

[5] Khataee A.R., Movafeghi A., Torbati S., SalehiLisar S.Y., Zarei M., Phytoremediation Potential of Duckweed (*Lemna Minor L.*) In Degradation of C.I. Acid Blue 92: Artificial Neural Network Modeling, *Ecotoxicol. Environ. Saf.*, **80**: 291–298 (2012).

[6] Fan L., Zhou Y., Yang W., Chen G., Yang F., Electrochemical Degradation of Aqueous Solution of Amaranth Azo Dye on ACF Under Potentiostatic Model, *Dyes Pigments*, **76**: 440–446 (2008).

[7] Wu J.S., Liu C.H., Chu K.H., Suen S.Y., Removal of Cationic Dye Methyl Violet 2B From Water by Cation Exchange Membranes, *J. Membr. Sci.*, **309**: 239–245 (2008).

[8] Woo Y.S., Rafatullah M., Al-Karkhi A.F.M., Tow T.T., Removal of Terasil Red R Dye by Using Fenton Oxidation: A Statistical Analysis, *Desal. Water Treat.*, **53**: 1–9 (2013).

[9] Azami M.S., Nawawi W.I., Ishak M.A.M., Ismail K., Ahmad Z., Jawad A.H., "Carbon Nitrogen Co-Doped P25: Parameter Study on Photodegradation of Reactive Red 4", *MATEC Web of Conferences*, **47**. EDP Sciences (2016).

[10] Nawawi W.I.W., Ain S.K., Zaharudin R., Jawad A.H., Ishak M.A.M., Ismail K., Sahid S., New TiO_2/DSAT Immobilization System for Photodegradation of Anionic and Cationic Dyes, *Int. J. Photoenergy* 2015(**3**): 1–6 (2015).

[11] Jawad A.H., Islam M.A., Hameed B.H., Cross-Linked Chitosan Thin Film Coated onto Glass Plate as an Effective Adsorbent for Adsorption of Reactive Orange 16, *Int. J. Biol. Macromolec*., **95**: 743–749 (2017).

[12] Jawad A.H., Sabar S., Ishak M.A.M., Wilson L.D., Norrahma S.S.A., Talari M.K., Farhan A.M., Microwave-Assisted Preparation of Mesoporous Activated Carbon From Coconut (*Cocos Nucifera*) Leaf by H_3PO_4-Activation for Methylene Blue Adsorption, *Chem. Eng. Commun*., **204**: 1143–1156 (2017).

[13] Foo K.Y., Hameed B.H., Potential of Jackfruit Peel as Precursor for Activated Carbon Prepared by Microwave Induced NaOH Activation, *Bioresour. Technol*., **112**: 143–150 (2012).

[14] Foo K.Y., Hameed B.H., Factors Affecting the Carbon Yield and Adsorption Capability of The Mangosteen Peel Activated Carbon Prepared by Microwave Assisted K_2CO_3 Activation, *Chem. Eng. J*., **180**: 66–74 (2012).

[15] Foo K.Y., Hameed B.H., Porous Structure and Adsorptive Properties of Pineapple Peel Based Activated Carbons Prepared Via Microwave Assisted KOH And K_2CO_3 Activation, *Microporous Mesoporous Mater*. **148**: 191–195 (2012).

[16] Dutta S., Bhattacharyya A., Ganguly A., Gupta S., Basu S., Application of Response Surface Methodology for Preparation of Low-Cost Adsorbent From Citrus Fruit Peel and for Removal of Methylene Blue, *Desalination*, **275**: 26–36 (2011).

[17] Arampatzidou A.C., Deliyanni E.A., Comparison of Activation Media and Pyrolysis Temperature for Activated Carbons Development by Pyrolysis of Potato Peels for Effective Adsorption of Endocrine Disruptor Bisphenol-A, *J. Colloid Interface Sci*., **466:** 101–112 (2016).

[18] Njoku V.O., Foo K.Y., Asif M., Hameed B.H., Preparation of Activated Carbons From Rambutan (*Nephelium Lappaceum*) Peel by Microwave-Induced KOH Activation for Acid Yellow 17 Dye Adsorption, *Chem. Eng. J*., **250**: 198–204 (2014).

[19] Ahmad M.A., Puad N.A.A., Bello O.S., Kinetic, Equilibrium and Thermodynamic Studies of Synthetic Dye Removal Using Pomegranate Peel Activated Carbon Prepared by Microwave-Induced KOH Activation, *Water Resour. Ind.*, **6**: 18–35 (2014).

[20] Pei Y.Y., Liu J.Y., Adsorption of Pb^{2+} In Wastewater Using Adsorbent Derived From Grapefruit Peel, *Adv. Mater. Res.*, **391–392**: 968–972 (2011).

[21] Owamah H.I., Biosorptive Removal of Pb(II) And Cu(II) From Wastewater Using Activated Carbon from Cassava Peels, *J. Mater. Cycles Waste Manage*., **16**: 347–358 (2014).

[22] Pandey R., Ansari N.G., Prasad R.L., Murthy R.C., Removal of Cd(II) Ions from Simulated Wastewater by HCl Modified *Cucumis Sativus* Peel: Equilibrium and Kinetic Study, *Air Soil Water Res*., **7**: 93–101 (2014).

[23] Bello O.S., Ahmad M.A., Semire B., Scavenging Malachite Green Dye from Aqueous Solutions Using Pomelo (*Citrus Grandis*) Peels: Kinetic, Equilibrium and Thermodynamic Studies, *Desal. Water Treat*., **56**: 521–535 (2015).

[24] Amela K., Hassen M.A., Kerroum D., Isotherm and Kinetics Study of Biosorption of Cationic Dye onto Banana Peel, *Energy Procedia*., **19**: 286–295 (2012).

[25] Singh P., Raizada P., Pathania D., Sharma G., Sharma P., Microwave Induced KOH Activation of Guava Peel Carbon as an Adsorbent for Congo Red Dye Removal From Aqueous Phase, *Indian J. Chem. Technol*., **20**: 305–311 (2013).

[26] Husein D.Z., Adsorption and Removal of Mercury Ions From Aqueous Solution Using Raw and Chemically Modified Egyptian Mandarin Peel, *Desalin. Water Treat*., **51**: 6761–6769 (2013).

[27] Jawad A.H., Mamat N.F.H., Fauzi M., Ismail K., Adsorption of Methylene Blue onto Acid-Treated Mango Peels : Kinetic, Equilibrium and Thermodynamic Study, *Desalin. Water Treat*., **59**: 210–219 (2017).

[28] Morton J.F., Orange, in: Morton, J.F., Ed., "Fruits of Warm Climates", Miami, pp. 134–142 (1987).

[29] Qiao Y., Xie B.J., Zhang Y., Zhang Y., Fan G., Yao X.L., Pan S.Y., Characterization of Aroma Active Compounds in Fruit Juice and Peel Oil of Jinchen Sweet Orange Fruit (*Citrus sinensis (L.) Osbeck*) by GC-MS and GC-O, *Molecules*, **13**: 1333-1344 (2008).

[30] Spreen T.H., "Projections of World Production and Consumption of Citrus to 2010. FAO Corporate Document Repository", *China/FAO Citrus Symposium Eng.* 14-17 May 2001 Beijing (China) Ministry of Agriculture, Beijing (China) eng.

[31] Okman I., Karagöz S., Tay T., Erdem M., Activated Carbons From Grape Seeds by Chemical Activation with Potassium Carbonate and Potassium Hydroxide, *Appl. Surf. Sci.*, **293**: 138–142 (2014).

[32] Hejazifar M., Azizian S., Sarikhani H., Li Q., Zhao D., Microwave Assisted Preparation of Efficient Activated Carbon From *Grapevine Rhytidome* for The Removal of Methyl Violet From Aqueous Solution, *J. Anal. Appl. Pyrolysis.*, **92**: 258–266 (2011).

[33] Gürses A., Doğar Ç., Karaca S.M., Ac¸ikyildiz M., Bayrak R., Production of Granular Activated Carbon From Waste *Rosa Canina* Sp. Seeds and Its Adsorption Characteristics for Dye, *J. Hazard. Mater.*, **131**: 254–259 (2006).

[34] Gerçel Ö., Özcan A., Özcan A.S., Gerçel H.F., Preparation of Activated Carbon From A Renewable Bio-Plant of *Euphorbia Rigida* by H_2SO_4 Activation and Its Adsorption Behavior In Aqueous Solutions, *Appl. Surf. Sci.*, **253**: 4843–4852 (2007).

[35] Low L.W., Teng T.T., Ahmad A., Morad N., Wong Y.S., A Novel Pretreatment Method of Lignocellulosic Material as Adsorbent and Kinetic Study of Dye Waste Adsorption, *Water Air and Soil Pollut.*, **218**: 293–306 (2011).

[36] Hasar H., Adsorption of Nickel (II) From Aqueous Solution onto Activated Carbon Prepared From Almond Husk, *J. Hazard. Mater.*, **97**: 49–57 (2003).

[37] Lata H., Garg V.K., Gupta R.K., Removal of A Basic Dye From Aqueous Solution by Adsorption Using *Parthenium Hysterophorus*: An Agricultural Waste, *Dyes Pigm.*, **74**: 653–658 (2007).

[38] Karagöz S., Tay T., Ucar S., Erdem M., Activated Carbons From Waste Biomass by Sulfuric Acid Activation and Their Use on Methylene Blue Adsorption, *Bioresour. Technol.*, **99**: 6214–6222 (2008).

[39] Royer B., Cardoso N.F., Lima E.C., Vaghetti J.C.P., Veses R.C., Applications of Brazalin Pine-Fruit Shell in Natural and Carbonized Forms as Adsorbents To Removal of Methylene Blue from Aqueous Solutions: Kinetics and Equilibrium Study, *J. Hazard. Mater.*, **164**: 1213–1222 (2009).

[40] Ho Y.S., Malaryvizhi R., Sulochana N., Equilibrium Isotherm Studies of Methylene Blue Adsorption onto Activated Carbon Prepared From *Delonix Regia* Pods, *J. Environ. Prot. Sci.*, **3**(1): 111–116 (2009).

[41] Swamy M.M., Nagabhushana B.M., Krishna R.H., Kottam N., Raveendra R.S., Prashanth P.A., Fast Adsorptive Removal of Methylene Blue Dye from Aqueous Solution onto a Wild Carrot Flower Activated Carbon: Isotherms and Kinetics Studies, *Desalin. Water Treat.*, **71**: 399–405 (2017).

[42] Jawad A.H., Rashid R.A., Ishak M.A.M., Wilson L.D., Adsorption of Methylene Blue onto Activated Carbon Developed From Biomass Waste by H_2SO_4 Activation: Kinetic, Equilibrium and Thermodynamic Studies, *Desalin. Water Treat.*, **57**: 25194–25206 (2016).

[43] Sharma N., Tiwari D.P., Singh S.K., The Efficiency Appraisal for Removal of Malachite Green by Potato Peel and Neem Bark: Isotherm and Kinetic Studies, *Int. J. Chem. Environ. Eng.*, **5**: 83–88 (2014).

[44] Garg V.K., Kumar R., Gupta R., Removal of Malachite Green Dye From Aqueous Solution by Adsorption Using Agro-Industry Waste: A Case Study of *Prosopis Cineraria*. *Dyes Pigments.*, **62**: 1–10 (2004).

[45] Auta M., Hameed B.H., Optimized Waste Tea Activated Carbon for Adsorption of Methylene Blue and Acid Blue 29 Dyes Using Response Surface Methodology, *Chem. Eng. J.*, **175**: 233– 243 (2011).

[46] Ahmedna M., Marshall W.E., Rao R.M., Clarke S.J., Use of Filtration and Buffers In Raw Sugar Colour Measurements, *J. Sci. Food Agric.*, **75**: 109–116 (1997).

[47] Adekola F.A., Adegoke H.I., Adsorption of Blue-Dye on Activated Carbons Produced From Rice Husk, Coconut Shell and Coconut Coir Pith, *Ife J. Sci.*, **7**: 151–157 (2005).

[48] ASTM Standard, Standard Test Method for Total Ash Content of Activated Carbon, Designation D2866-94, (2000).

[49] "Lubrizol Standard Test Method, Iodine Value, Test Procedure AATM 1112-01", October 16 (2006).

[50] Lopez-Ramon M.V., Stoeckli F., Moreno-Castilla C., Carrasco-Marin F., On The Characterization of Acidic And Basic Surface Sites on Carbons by Various Techniques, *Carbon.*, **37**: 1215– 1221 (1999).

[51] Jawad A.H., Ishak M.A.M., Farhan A.M., Ismail K., Response Surface Methodology Approach for Optimization of Color Removal and COD Reduction of Methylene Blue Using Microwave-Induced NaOH Activated Carbon from Biomass Waste, *Desalin. Water Treat.*, **62**: 208–220 (2017).

[52] Jawad A.H., Rashid R.A., Ismail K., Sabar S., High Surface Area Mesoporous Activated Carbon Developed from Coconut Leaf by Chemical Activation with H_3PO_4 for Adsorption of Methylene Blue, *Desalin. Water Treat*., **74**: 326–335 (2017).

[53] Rashid R.A., Jawad A.H., Ishak M.A.M., Kasim N.N., KOH-Activated Carbon Developed from Biomass Waste: Adsorption Equilibrium, Kinetic and Thermodynamic Studies for Methylene Blue Uptake, *Desalin. Water Treat*., **57**: 27226–27236 (2016).

[54] Jawad A.H., Nawi M.A., Characterizations of the Photocatalytically-Oxidized Cross-Linked Chitosan-Glutaraldehyde and its Application as a Sub-Layer in the TiO_2/CS-GLA Bilayer Photocatalyst System, *J. Polym. Environ.*, **20**: 817-829 (2012).

[55] Islam M.A., Ahmed M.J., Khanday W.A., Asif M., Hameed B.H., Mesoporous Activated Carbon Prepared from NaOH Activation of Rattan (*Lacosperma Secundiflorum*) Hydrochar for Methylene Blue Removal, *Ecotoxicol. Environ. Saf*., **138**: 279–285 (2017).

[56] Rashid R.A., Jawad A.H., Ishak M.A.M., Kasim N.N., $FeCl_3$ -Activated Carbon Developed from Coconut Leaves: Characterization and Application for Methylene Blue Removal, *Sains Malaysiana*, 47(**3**): 603–610 (2018).

[57] Bedin K.C., Martins A.C., Cazetta A.L., Pezoti O., Almeida V.C., KOH-Activated Carbon Prepared From Sucrose Spherical Carbon: Adsorption Equilibrium, Kinetic and Thermodynamic Studies for Methylene Blue Removal, *Chem. Eng. J.*, **286**: 476–484 (2015).

[58] Tsai W.T., Lai C.W., Hsien K.J., Adsorption Kinetics of Herbicide Paraquat from Aqueous Solution onto Activated Bleaching Earth, *Chemosphere*., **55**: 829–837 (2004).

[59] Ofomaja A.E., Sorption Dynamics and Isotherm Studies of Methylene Blue Uptake on to Palm Kernel Fibre, *Chem. Eng. J*., **126**: 35–43 (2007).

[60] Hossein F., Ali Akbar M.A., Arezomand S., Reza H., Hossein M.A., Kinetics and Equilibrium Studies of The Removal Of Blue Basic 41 and Methylene Blue From Aqueous Solution Using Rice Stems, *Iran. J. Chem. Chem. Eng. (IJCCE)*, **34**(3): 33-42 (2015).

[61] Langmuir I., The Adsorption of Gases on Plane Surfaces of Glass, Mica and Platinum, *J. Am. Chem. Soc*., **40**: 1361–1403 (1918).

[62] Hall K.R., Eagleton L.C., Acrivos A., Vermeulen T., Pore- and Solid Diffusion Kinetics in Fixed-Bed Biosorption Under Constant-Pattern Conditions, *Ind. Eng. Chem. Fundam.*, 5 212–223 (1966).

[63] Freundlich H., Ueber Die Adsorption In Loesungen (Adsorption in Solution), *Z. Phys. Chem.*, **57**: 385–470 (1906).

[64] Temkin M.J., Pyzhev V., Recent Modifications to Langmuir Isotherms, *Acta Physiochim. USSR*, **12**: 217–222 (1940).

[65] Pathania D., Sharma S., Singh P., Removal of Methylene Blue by Adsorption onto Activated Carbon Developed From *Ficus Carica* Bast, *Arab. J. Chem*., **10**(1): 1445–1451 (2017).

[66] Lagergren S., Zur Theorie Der Sogenannten Adsorption Geloster Stoffe, *K. Sven. Vetenskapsakad. Handl*., **24**: 1–39 (1898).

[67] Ho Y.S., McKay G., Sorption of Dye From Aqueous Solution by Peat, *Chem. Eng. J*., **70**: 115–124 (1998).

[68] Karaçetin G., Sivrikaya S., Imamoğlu M., Adsorption of Methylene Blue from Aqueous Solutions by Activated Carbon Prepared From Hazelnut Husk Using Zinc Chloride, *J. Anal. Appl. Pyrolysis*, **110**: 270–276 (2014).

[69] Jaycock M.J., Parfitt, G.D., "Chemistry of Interfaces", Ellis Horwood Ltd., Onichester, (1981).

[70] Noll K.E., Gounaris V., Hou W.S., "Adsorption Technology for Air and Water Pollution Control", Lewis Publishers, Chelsea, MI, 21–22 (1992).

[71] Ghaedi M., Shokrollahi A., Tavallali H., Shojaiepoor F., Keshavarz B., Hossainian H., Soylak M., Purkait M.K., Activated Carbon and Multiwalled Carbon Nanotubes as Efficient Adsorbents for Removal of Arsenazo (III) and Methyl Red from Waste Water, *Toxicol. Environ. Chem.*, **93**(3): 438–449 (2011).

[72] Asouhidou D.D., Triantafyllidis K.S., Lazaridis N.K., Matis K.A., Kim S.S., Pinnavaia T.J., Sorption of Reactive Dyes from Aqueous Solutions by Ordered Hexagonal and Disordered Mesoporous Carbons, *Micropor. Mesopor. Mate*r., **117**: 257–267 (2009).

[73] Gundogdu A., Duran C., Senturk H.B., Soylak M., Ozdes D., Serencam H., Imamoglu M., Adsorption of Phenol from Aqueous Solution on a Low-Cost Activated Carbon Produced From Tea Industry Waste: Equilibrium, Kinetic, and Thermodynamic Study, *J. Chem. Eng. Data*., **57**(10): 2733-2743 (2012).